p38α in CD11c$^+$ cells drives sex-specific differences during progression of autoimmune demyelination

Running title: p38α controls CNS infiltration in males

Olga V. Chechneva[1,2*], Florian Mayrhofer[2], Zhanna Dariychuk[2], Anthony Zhen[2], David Pleasure[2], Wenbin Deng[1,2*]

[1]Department of Biochemistry and Molecular Medicine, UC Davis, Sacramento, CA 95817; [2]IPRM, Shriners Hospital for Children, Sacramento, CA 95817

Corresponding authors:

Olga V. Chechneva

Department of Biochemistry and Molecular Medicine

School of Medicine, UC Davis

2425 Stockton Blvd, Sacramento, CA, 96817

Phone: 916-453-2250

Fax: 916-453-2288

Email: chechneva@gmail.com

Wenbin Deng

Department of Biochemistry and Molecular Medicine

School of Medicine, UC Davis

2425 Stockton Blvd, Sacramento, CA, 96817

Phone: 916-453-2287

Fax: 916-453-2288

Email: wbdeng@ucdavis.edu

Abstract

Multiple sclerosis (MS) is an autoimmune demyelinating disorder developing with higher prevalence in women than men, while accelerated MS progression is evident in men. Mechanisms underlying sexual dimorphism in MS remain unclear. Here, we found that although female and male mice with conditional knockout of *p38α* in $CD11c^+$ cells initially developed attenuated clinical symptoms of experimental autoimmune encephalomyelitis (EAE), an animal model of MS, as has been shown earlier, female mice underwent spontaneous disease progression after day 30 post EAE induction. EAE progression in females was associated with T lymphocyte and macrophage infiltration into the CNS parenchyma. In contrast, male mice with CD11c cell specific *p38a* deficiency were protected from disease progression as immune cells were trapped within perivascular spaces without entering parenchyma. We identified male-specific p38α signaling in $CD11c^+CD11b^+Iba1^+$ cells to control immune cell infiltration and progression of autoimmune demyelination. These findings advance our understanding of sex-biased mechanisms in MS relapse and progression and provide new rationale for the development of sex-specific MS therapies.

Keywords: multiple sclerosis progression, experimental autoimmune encephalomyelitis, $CD11c^+$ cells, macrophages, microglia

Abbreviations: APC, antigen presenting cells; CD40LG, CD40 ligand; CNS, central nervous system; DC, dendritic cells; EAE, experimental autoimmune encephalomyelitis; eGFP, enhanced green fluorescent protein; GFAP, glial fibrillary acidic protein; Iba1, ionized calcium binding adaptor molecule 1; MBP, myelin basic protein; MHC-II, major histocompatibility complex-II; MOG_{35-55}, myelin oligodendrocyte glycoprotein 35-55; MS, multiple sclerosis; OPN, osteopontin; PBS, phosphate buffered saline; PTX, pertussis toxin; T_H, T helper.

Introduction

MS is an autoimmune demyelinating disorder characterized by chronic inflammation, myelin loss and axonal degeneration affecting young adults. MS displays a dynamic clinical phenotype with the most common appearance as a relapsing-remitting form progressing over time. EAE is the most commonly used animal model of MS. Re-activation of myelin-reactive T cells by antigen presenting cells (APC) within the target organ is essential for EAE relapse and progression (Chastain et al, 2011). The APC-T cell interaction through CD40-CD40 ligand (CD40LG) and secretion of IL-12 by APC have been shown to mediate re-activation of T helper (T_H) type 1 cells and progression of MS (Balashov et al, 1997). Recent studies demonstrated the involvement of T_H17 cells in MS relapse and progression (Babaloo et al, 2015; Romme Christensen et al, 2013).

Dendritic cells (DC), B cells, macrophages and microglia are professional APC that can process and present antigens via major histocompatibility complex-II (MHC-II) molecules to T cells (Chastain et al, 2011; Molnarfi et al, 2013). In adoptive transfer EAE, $CD11c^+$ DC found in the CNS meninges or perivascular sites are able to reactivate myelin-primed T cells causing clinical symptoms of MS (Greter et al, 2005). CD11c is the integrin alpha X chain protein (encoded by *Itgax* gene), that is expressed by DC and some macrophages, as DC and macrophages share a common progenitor (Merad et al, 2013). Microglia initiate CD11c expression in response to injury. $CD11c^+$ microglia are found preceding the onset of EAE clinical symptoms where they constitute 30% of microglia population (Fischer & Reichmann, 2001; Serafini et al, 2000). The role of $CD11c^+$ macrophages and microglia in EAE is unknown.

MS displays a sexual bias and develops with higher prevalence in women, while men demonstrate more rapid disease progression (Gourraud et al, 2012; Voskuhl & Gold, 2012). Sexual dimorphism in MS has been linked to hormonal, genetic and environmental factors (Li et al, 2017; Voskuhl & Gold,

2012). Still, signaling pathways and cellular mechanisms regulating MS relapse and progression and sex-specific differences are not well understood.

The p38α MAPK (encoded by *Mapk14* gene) is a central regulator of stress and inflammation in multiple cell types (Zarubin & Han, 2005). Current reports demonstrated that $CD11c^+$ DC require p38a to control T_H cells differentiation toward T_H17 phenotype to induce and sustain myelin-specific T cell reactivity (Di Mitri et al, 2015; Huang et al, 2012). Knockout of *p38a* in $CD11c^+$ DC, results in a significant reduction of EAE clinical symptoms (Huang et al, 2012; Krementsov et al, 2014). A sex-dependent role of p38α signaling in myeloid cells has been demonstrated, where pharmacological inhibition or myeloid cell knockout of p38α reduce EAE clinical symptoms and inflammation in female but not male mice (Krementsov et al, 2014). The role of p38a in MS relapse and progression is unknown.

Immunization of C57BL/6 mice with myelin oligodendrocyte glycoprotein 35-55 (MOG_{35-55}) induces a chronic-progressive form of EAE where slight remission after the peak is followed by relapse transitioning into chronic EAE without noticeable sexual differences (Chechneva et al, 2011; Rahn et al, 2014). Here we report that while initially protected from MOG-induced autoimmune demyelination, female mice with *CD11c* promoter-driven conditional knockout of *p38α* in $CD11c^+$ cells ($p38\alpha^{\Delta CD11c}$) develop spontaneous EAE progression in contrast to $p38\alpha^{\Delta CD11c}$ males. EAE progression in females was associated with CNS infiltration of T cells and macrophages. We identified $CD11c^+CD11b^+Iba1^+$ cells to control immune cell infiltration and EAE progression through p38α signaling in males.

Results

Knockout of *p38α* in CD11c$^+$ cells prevents EAE progression in male mice

p38α MAPK in CD11c$^+$ cells controls generation of myelin-specific T_H17 cells involved in the development of severe EAE. The role of p38α MAPK in EAE progression is unknown. We induced EAE by MOG immunization in male and female *p38α*$^{\Delta CD11c}$ mice and *p38α*$^{fl/fl}$ controls. *p38α*$^{fl/fl}$ mice developed instant severe EAE with no sex-dependent differences during disease course (Fig. 1A, Table 1). Both, male and female *p38α*$^{\Delta CD11c}$ mice initially displayed attenuated EAE clinical symptoms compared to controls (Fig. 1A, Table 1), as has been reported earlier (Huang et al, 2012; Krementsov et al, 2014). However, at day 30-35 post immunization, 72% of *p38α*$^{\Delta CD11c}$ females developed spontaneous clinical relapse and progression (Fig. 1A, Table 1). We investigated the pathology of relapse and progression in *p38α*$^{\Delta CD11c}$ female compared to *p38α*$^{\Delta CD11c}$ male mice. Histological analysis using H&E and LFB & Cresyl Violet revealed increased infiltration and demyelination in the ventral, dorsal and lateral lumbar spinal cord of *p38α*$^{\Delta CD11c}$ females compared to males (Fig. 1B, C, E). Infiltration and myelin loss were confirmed by DAPI nuclear marker and MBP staining (Fig. 1D). We conclude that in males EAE relapse and progression is dependent on p38α MAPK signaling in CD11c$^+$ cells.

Knockout of *p38α* in CD11c$^+$ cells in males prevents CNS infiltration of T cells and macrophages

Damage to oligodendrocytes in autoimmune demyelination is initiated by infiltrating effector cells, such as myelin-specific T cells (Gold et al, 2006) and macrophages (Ajami et al, 2011). We found an increased number of CD4$^+$ T cells in the lumbar spinal cord parenchyma of female *p38α*$^{\Delta CD11c}$ mice compared to males (Fig. 2A-B). In females, CD4$^+$ cells were scattered throughout the entire white

matter parenchyma (Fig. 2B, enlargement). In contrast, in *p38α*$^{\Delta CD11c}$ males, CD4^{+} T cells were found in perivascular clusters (Fig. 2A, enlargement). Single CD4^{+} cells were still detected within the parenchyma in males (Fig. 2A, enlargement). FACS and PCR analysis of lumbar spinal cord revealed no significant differences in protein expression and mRNA level of CD4 and CD8a (Fig. 2D-F). T_H1 and T_H17 CD4^{+} cells are involved in MS and EAE and express INF-γ and IL-17, respectively (Babaloo et al, 2015; Balashov et al, 1997; Romme Christensen et al, 2013). We found an increased level of *INF-γ* mRNA in the lumbar spinal cord of female mice (Fig. 2G). The level of *IL-17a* mRNA was not significantly elevated in females compared to males (Fig. 2G). Generation of T_H1 and T_H17 CD4^{+} cells is controlled by APC-derived cytokines. Increase in transcription level of *IL-12b* (also known as *IL-12p40*) , a driver of T_H1 cells differentiation (Balashov et al, 1997), was found in the lumbar spinal cords of female mice at EAE progression (Fig. 2H). No differences in transcription levels of *IL-6*, a cytokine promoting generation of T_H17 cells (Heink et al, 2017), were found between female and male mice (Fig. 2I). Our data indicate that p38α in CD11c^{+} cells alters T cell invasion into the parenchyma in males.

Next, we used immunohistochemistry to characterize the pattern of infiltration in *p38α*$^{\Delta CD11c}$ female and male mice. In males, we found Iba1^{+} or lectin^{+} macrophages localized and clustered along perivascular spaces and meninges (Fig. 3A, C). However, in females, macrophages/reactive microglia were scattered throughout the entire white matter (Fig. 3B, D). Analysis of CD45 expression confirmed reduced immune cell infiltration in males compared to females (Fig. 3E-F). Ramified Iba1^{+} microglia were morphologically distinguishable in males, compared to Iba1^{+} macrophages/reactive microglia found in females. Upregulation of *CD45* and *CD11b* (*Itgam* gene) mRNA was found in the spinal cords of *p38α*$^{\Delta CD11c}$ females (Fig. 3G-H). Our data show that macrophage infiltration contributes to EAE relapse and progression and is dependent on p38α signaling in CD11c^{+} cells only in males.

CD11c$^+$CD11b$^+$Iba1$^+$ cells are involved in EAE progression in *p38α*$^{\Delta CD11c}$ females

We next examined the presence and distribution of CD11c$^+$ cells in EAE spinal cords of *p38α*$^{\Delta CD11c}$ male and female mice. Commercially available antibodies were not able to detect CD11c$^+$ cells by immunohistochemistry, likely due to low expression of CD11c in migrating and activated DC (Merad et al, 2013; Prodinger et al, 2011). Our transgenic mice express eGFP under the *CD11c* promoter, therefore, we used eGFP expression to track CD11c$^+$ cells in EAE spinal cords. In males, we found eGFP$^+$ cells clustered at the meninges and perivascular spaces (Fig. 4A). These cells strongly expressed macrophage/microglia marker CD11b. Some eGFP$^+$ reactive microglia with intermediate expression of CD11b (Fig. 4A, arrow) and eGFP$^+$CD11b$^+$ cells with morphology of DC (referred to as DC-like CD11c$^+$ microglia; Fig. 4A, arrowhead) were found within the spinal cord parenchyma in *p38α*$^{\Delta CD11c}$ males. In females, eGFP$^+$CD11b$^+$ cells with macrophage/reactive microglia morphology were found in the perivascular spaces and within the spinal cord parenchyma (Fig. 4B). To differentiate DC from macrophages, we co-stained eGFP$^+$ cells with macrophage/microglia marker Iba1. We found that most of the eGFP$^+$ microglia in males and eGFP$^+$ macrophages/reactive microglia in females expressed Iba1 (Fig. 4C-D). A higher level of *CD11c* mRNA was detected in the lumbar spinal cords of *p38α*$^{\Delta CD11c}$ females (Fig. 4E), indicating an increase in CD11c$^+$ cell number. Our data suggest that (i) CD11c$^+$CD11b$^+$Iba1$^+$ cells control CNS immune cells infiltration in EAE progression and (ii) their function is dependent on p38α signaling in males.

Macrophages/reactive microglia upregulate CD40 and MHC-II in *p38α*$^{\Delta CD11c}$ female mice

Interaction of co-stimulatory molecule CD40 on APC with CD40LG on T cells regulates release of IL-12 by APC (Yanagawa & Onoe, 2006), T cell reactivation and EAE progression (Becher et al, 2001). Moreover, increase in CD40LG is found in patients with progressive form of MS (Balashov et al,

1997). Analysis of mRNA transcription level of *CD40LG* in the lumbar spinal cord showed no significant differences between *p38α*$^{\Delta CD11c}$ females and males at EAE progression (Fig. 5A). Next, we questioned whether lack of *p38α* in CD11c^{+} cells alters the expression of CD40. The mRNA level of *CD40* was significantly increased in female mice (Fig. 5B). Notably, CD40 protein expression was dramatically upregulated and found in perivascular macrophages and parenchymal macrophages/reactive microglia throughout the entire spinal cord in females (Fig. 5E-F). In males, expression of CD40 was evident in clustered perivascular and meningeal macrophages (Fig. 5C-D). Low CD40 expression was found in the parenchyma, in association with ramified microglia.

We next examined the effect of *p38α* knockout on MHC-II expression in CD11c^{+} cells. In males, most of MHC-II^{+} cells were localized to the perivascular spaces where we found eGFP^{+}MHC-II^{+}Iba1^{+} and eGFP^{-}MHC-II^{+}Iba1^{+} macrophages (Fig. 5G) and eGFP^{+}MHC-II^{+}Iba1^{-} DC (Fig. 5G, arrow). Low expression of MHC-II was found in eGFP^{+}Iba1^{+} microglia (Fig. 5G) and DC-like CD11c^{+} microglia (Fig. 5G, asterisk). In males, we also identified eGFP^{+}Iba1^{+} microglia that were MHC-II^{-} (Fig. 5G, pound) and eGFP^{+} cells lacking expression of Iba1 and MHC-II (Fig. 5G, arrowhead). MHC-II expression was increased in females, where most of the eGFP^{+}Iba1^{+} cells co-expressed MHC-II and were present in the perivascular spaces and parenchyma (Fig. 5H). Our data indicate that lack of *p38α* does not alter expression of CD40 or MHC-II in CD11c^{+} cells and increase in CD40 and MHC-II expression in *p38α*$^{\Delta CD11c}$ females is caused by increase in macrophage infiltration and microglia reactivity.

Astrocyte-derived OPN and CCL2 mediate EAE progression in *p38α*$^{\Delta CD11c}$ females

OPN has been shown to enhance T cell survival, immune cell infiltration and EAE relapse and progression (Hur et al, 2007). We found increased OPN (*Spp1* gene) expression in *p38α*$^{\Delta CD11c}$ females

compared to males (Fig. 6A-C). We next examined the cellular origin of OPN in male and female lumbar spinal cords. We used lectin to label infiltrating macrophages, microglia and vascular endothelium. We found that in male (Fig. 6D) and female (Fig. 6E) lumbar spinal cords, OPN expression was preferentially localized to $GFAP^+$ astrocytes. Hypertrophic, reactive astrocytes were apparent in *p38α*$^{\Delta CD11c}$ females. Interestingly, OPN^+ cells with morphology of oligodendrocyte precursor cells were present in the spinal cords of *p38α*$^{\Delta CD11c}$ male mice (Fig. 6D, arrows). Astrocyte-derived CCL2 is required for macrophage trafficking into the CNS parenchyma (Kim et al, 2014; Moreno et al, 2014). We found increase in CCL2 protein expression in reactive astrocytes in females vs males (Fig. 6 F-G). Significant increase in *CCL2* mRNA in the lumbar spinal cords of *p38α*$^{\Delta CD11c}$ females compared to males was observed (Fig. 6H). No significant differences in the transcription level of *CCR2*, a CCL2 chemokine receptor expressed in infiltrating macrophages (Ajami et al, 2011), were found (Fig. 6I). Our data suggest that p38α signaling in $CD11c^+$ cells is involved in astrocyte-controlled CNS infiltration, but only in males.

Discussion

The mechanism of MS relapse and progression and its sexual bias remain poorly understood. Here we report that, although protected at the initial phase of disease, female mice lacking p38α in $CD11c^+$ cells developed spontaneous relapse and progression of EAE clinical symptoms in contrast to male cohorts that remained protected. Protection in *p38α*$^{\Delta CD11c}$ males was due to the failure of T cells and macrophages to enter CNS parenchyma.

Reactivation of myelin-reactive T cells by APC is required to recognize their target and permit CNS parenchymal entry (Larochelle et al, 2011). T cell reactivation takes place in perivascular spaces, from where activated cells cross the endothelial basement membrane and glial limitans, a layer formed by astrocyte end-feet, to enter CNS parenchyma (Owens et al, 2008). We found that disease progression

in *p38α*$^{\Delta CD11c}$ females concurred with active invasion of CD4^{+} T cells and macrophages into the spinal cord parenchyma. In contrast, in *p38α*$^{\Delta CD11c}$ males, T cells and macrophages clustered along perivascular spaces with limited parenchymal presence of T cells. Based on morphology, only few macrophages were found in the spinal cord parenchyma in males. Our findings indicate that during EAE progression CD11c^{+} cells control immune cell infiltration into the CNS parenchyma and in males, it involves p38α signaling.

There are three CD11c^{+} cell populations that can be responsible for immune cell CNS trafficking at EAE progression: (i) DC, (ii) macrophages, (iii) microglia. Greter et al. reported that perivascular CD11c^{+} DC are indispensable for CNS immune cell invasion and require MHC-II expression to induce EAE clinical symptoms (Greter et al, 2005). We found that most of the CD11c^{+} cells in the perivascular spaces in *p38α*$^{\Delta CD11c}$ males and females and in the spinal cord parenchyma in *p38α*$^{\Delta CD11c}$ females co-expressed macrophage/microglia markers CD11b and Iba1 and identified them as macrophages. Myeloid DC co-express CD11b and infiltrate CNS parenchyma during EAE (Dogan et al, 2008). Expression of Iba1 by myeloid DC has not been reported.

Importantly, only a subset of CD11b^{+}Iba1^{+} macrophages co-expressed CD11c. CD11c expression in macrophages is linked to pro-inflammatory M1 phenotype (Wentworth et al, 2010). Macrophage infiltration induces exacerbation of EAE clinical symptoms (Ajami et al, 2011; Dogan et al, 2008) and therapeutic depletion of macrophages was shown to inhibit lymphocyte CNS invasion (Moreno et al, 2016), specifically their ability to cross the glial limitans (Tran et al, 1998). Notably, CD11c^{+}CD11b^{+}Iba1^{+} macrophages were found in sciatic nerve inflammatory infiltrated before the onset and at the peak of experimental autoimmune neuritis (Pashenkov et al, 2000). These evidences suggest that CD11c^{+}CD11b^{+}Iba1^{+} macrophage subtype, is critical in CNS infiltration during EAE progression.

In females, CD11c$^+$ reactive microglia were morphologically indistinguishable from macrophages. In males, we found CD11c$^+$CD11b$^+$Iba1$^+$ microglia with DC phenotype in addition to CD11c$^+$CD11b$^+$Iba1$^+$ partially activated and CD11c$^+$CD11b$^+$Iba1$^+$ ramified microglia. The origin of DC-like CD11c$^+$ microglia and whether they are key regulators of CNS infiltration and EAE progression remain unclear. Microglia originate from the yolk sac during embryonic development and maintain their population by self-renewal throughout life (Alliot et al, 1999; Huang et al, 2018). The presence of CNS-derived DC-like CD11c$^+$ microglia was reported in the spinal cord, brain and optic nerve parenchyma in healthy mice expressing GFP under the control of *CD11c* promoter (Prodinger et al, 2011). We could detect a low expression of MHC-II in DC-like CD11c$^+$ microglia that suggests a possible role in reactivating perivascular myelin-reactive T cells *in vivo*. However, it has been shown that CNS specific MHC-II knockout fails to protect mice from adoptive transfer EAE (Greter et al, 2005), pointing toward an antigen presentation-independent function of CD11c$^+$ DC-like microglia in EAE. Indeed, Prodinger et al. showed that in the healthy CNS, processes of DC-like CD11c$^+$ microglia localize in close proximity to glial limitans, suggesting their role in astrocyte glial limitans organization (Prodinger et al, 2011). Noteworthy, in female mice in EAE progression, we found hypertrophic reactive astrocytes to strongly express OPN, that is also upregulated in the plasma of MS patients before relapse (Vogt et al, 2004) and implicated in macrophage infiltration (Bruemmer et al, 2003; Giachelli et al, 1998), T cell survival and worsening of EAE clinical symptoms (Hur et al, 2007). Female reactive astrocytes also overexpressed CCL2, a macrophage attracting chemokine (Kim et al, 2014; Moreno et al, 2014). The interaction of DC-like CD11c$^+$ microglia with astrocytes and CNS immune cell trafficking need to be further investigated. Regular microglia with ramified or partially activated phenotype in males and activated microglia in females expressed CD11c and need to be viewed as an additional candidate to control CNS immune cell infiltration and EAE progression.

Interaction of CD40 on APC with CD40LG on T cells is critical for T cell reactivation (Becher et al, 2001) involving p38 MAPK signaling (Yanagawa & Onoe, 2006). A sex-dependent role of this interaction is linked to the CD40LG gene which is located on the X-chromosome (Wang et al, 2016). We found no differences in CD40LG mRNA between males and females during EAE progression. In females, increased expression of CD40 was associated with infiltrating macrophages/reactive microglia. In males, $CD40^{+}$ perivascular macrophages and parenchymal microglia were present without causing disease exacerbation. These findings suggest that lack of p38α in $CD11c^{+}$ cells does not alter the expression of CD40LG or CD40. However, whether it alters CD40-CD40LG interaction is still unknown.

p38 MAPK signaling is involved in sex-biased immune response. In microglia, p38α signaling was identified as a cause of neuropathic and inflammatory pain in male but not female mice and rats with chronic constriction injury (Taves et al, 2016). MAPK-activated kinase 2, a substrate for p38 MAPK, was found to regulate osteoclastogenesis only in males (Herbert et al, 2015). Testosterone-dependent increase in p38 phosphorylation in splenic and peritoneal macrophages was found in male mice after trauma-hemorrhage (Angele et al, 2003). Interestingly, pharmacological inhibition of p38 signaling and knockout of *p38α* in $LyzM^{+}$ myeloid cells ($p38\alpha^{\Delta LyzM}$), that include monocytes, macrophages and granulocytes, was effective to reduce EAE clinical symptoms at the acute phase in females but not males (Krementsov et al, 2014). Here we showed that only in male mice knockout of *p38α* in $CD11c^{+}$ cells, including DC, macrophages and microglia, was effective to reduce CNS immune cell infiltration and EAE progression. Notably, the degree of immune cell activation defined by EAE induction model may alter the cell-specific role of *p38α* signaling. MOG-PTX used in our study causes severe EAE. Neuroprotection in $p38\alpha^{\Delta LyzM}$ females was observed in a PTX–free (2xMOG) model with less severe disease outcome, whereas in MOG-PTX model, neuroprotection was not evident in $p38\alpha^{\Delta LyzM}$ females

(Krementsov et al, 2014). Furthermore, the cell-specific role of p38α at the acute EAE phase, compared to relapse/progression developing on the base of chronic inflammation are likely distinct. In support, a pro-inflammatory and anti-inflammatory role of p38α in dermal macrophages was demonstrated in chronic and acute, respectively, skin injury (Kim et al, 2008). Moreover, neurons have been shown to upregulate LyzM expression in neurodegenerative conditions (Orthgiess et al, 2016). The sex-dependent role of p38α in neurons has not been investigated so far.

For more than a decade, p38α signaling has been viewed as an attractive target to treat auto-immune and inflammatory disorders (Herlaar & Brown, 1999) with an emerged role in MS. Yet, many p38 MAPK inhibitors failed to fulfill their expectations in clinic, possibly due to diverse functions of p38α kinase depending on the cell type, nature of stimulatory factor (Angele et al, 2003; Krementsov et al, 2013), together with possible cell-specific epigenetic regulation (Kaminska et al, 2016) and the effect of gut bacteria metabolites (Haghikia et al, 2015). Here we showed, that p38α signaling in $CD11c^+$ cells is involved in immune cell infiltration and progression of autoimmune demyelination in males. In females, parenchymal entry of immune cells and EAE progression are p38α independent, and rely on an alternative signaling pathway, where NF-κB can be suggested as a possible candidate (Yanagawa & Onoe, 2006). These findings advance our understanding of sex-biased mechanisms of EAE relapse and progression and provide rationale to the development of sex-specific therapeutic strategies for MS.

Materials and Methods

Animals

Mice carrying the *p38α* floxed allele [B6.129-*Mapk14*<tm1.2Otsu.] were crossed with mice expressing Cre recombinase under the *CD11c* promoter (C57BL/6J-Tg(*Itgax*-cre-EGFP)4097Ach/J, JAX stock #007567). The offspring were genotyped for the presence of *p38α* floxed allele and Cre insert as described earlier (Lo et al, 2014). Mice homozygous for the *p38α* floxed allele were classified into

male and female *p38α*$^{\Delta CD11c}$ (Cre-positive) and *p38α*$^{fl/fl}$ (Cre-negative). Mice were maintained in accordance to the NIH Guide for the Care and Use of Laboratory Animals. Experimental protocols were approved by the Institutional Animal Care and Use Committee at the University of California, Davis.

EAE induction

EAE was induced in *p38α*$^{\Delta CD11c}$ and *p38α*$^{fl/fl}$ mice of both sexes at the age of 9-12 weeks as described earlier (Chechneva et al, 2011). In brief, mice were injected subcutaneously at two flank sites with an emulsion of 300 µg of MOG_{35-55} (New England Peptide) in incomplete Freund's adjuvant supplemented with 500 µg Mycobacterium tuberculosis H37Ra (Difco). Mice received 200 ng of PTX (pertussis toxin) (List Biological Labs) intraperitoneally on day 0 and 2. The severity of clinical symptoms was evaluated using the standard neurological scoring system for EAE: 0 - no deficit; 0.5 - mild loss of tail tone; 1 - complete loss of tail tone; 1.5 - mildly impaired righting reflex; 2 - abnormal gait (ataxia) and/or impaired righting reflex; 2.5- single hind limb paresis and ataxia; 3 - double hind limb paresis; 3.5 - single limb paralysis and paresis of second limb / paresis of both hind limbs and weakness of front limbs; 4 - full paralysis of two limbs; 4.5 - hind limb paralysis with hind body paresis; 5 – moribund or death.

Histology and pathological scoring

Histological analysis was performed as described earlier (Chechneva et al, 2011). Briefly, mice were anesthetized with isoflurane and perfused with ice cold PBS (phosphate buffered saline). Lumbar spinal cords were dissected, cryopreserved and cut in 15 µm sections on the cryostat. For H&E (Hematoxylin & Eosin) staining sections were stained with Mayer's hematoxylin followed by 1% eosin. For LFB (Luxol Fast Blue) staining, sections were incubated with 0.1% LFB solution at 60^0C

for 16 h followed by differentiation with 0.05% lithium carbonate and co-stained with 0.1% Cresyl Violet. Slides were mounted using Cytoseal-60 medium and images were acquired on Keyence BZ-9000 microscope. For pathological analysis, per animal, six sections of the lumbar spinal cord collected in the interval of 180 µm were scored by blinded investigator for infiltration and demyelination as previously described (Shi et al, 2011).

Immunohistochemistry

For immunostaining, sections were washed with PBS to remove excess of cryoprotectant. Nonspecific binding of antibodies was blocked using 10% normal serum in 0.1% Triton-X in PBS. Samples were then incubated with rat anti-MBP (myelin basic protein; 1:5; Millipore MAB395), rabbit anti-Iba1 (ionized calcium binding adaptor molecule 1; 1:500; Wako 019-19741), rabbit anti-CD4 (1:200; Abcam ab183685), rat anti-CD45 (1:200; SouthernBiotec 1660-01), chicken anti-GFAP (glial fibrillary acidic protein; 1:500; Aves GFAP), FITC conjugated lectin from Lens culinaris (1:300; Sigma), chicken anti-GFP (1:500, Abcam ab13970), mouse anti-CD40 (1:200; Novus NBP1-43416), rat anti-CD11b (1:100, BD Pharmingen 550282), rabbit anti-osteopontin (OPN; 1:200, Abcam ab8448), rabbit anti-CCL2 (1:200, AB1834), rat anti-MHC-II (1:100; eBiosciences 14-5321-85) overnight at 4 °C. For fluorescent staining, slides were washed in PBS and incubated with fluorophore-conjugated secondary antibody Alexa Fluor 488, 555 or 647 (1:1000; Life Technologies). Slides were mounted using DAPI Fluoromount-G (SouthernBiotech). Images were acquired on Nikon Eclipse TE 2000-E microscope using a D-Eclipse C1si camera (Nikon). For DAB staining, slides were washed in PBS and incubated with HRP-conjugated secondary antibody. Positive signal was visualized using ImmPACT DAB Peroxidase substrate kit (Vector labs). Images were acquired on Olympus BX61-DSU microscope using Hamamatsu ORCA-ER camera (Hamamatsu Photonics). For fluorescent and DAB staining

negative controls omitting primary antibody were performed. Images were processed using Adobe Photoshop CC.

FACS analysis

Mice were transcardially perfused with ice-cold PBS. Brains and spinal cords were dissected and placed in ice-cold HBSS (Hank's Balanced Salt Solution) supplemented with 2 mg/ml collagenase D (Roche) and 100 U/ml DNAse I (Worthington). For single cell suspension, tissue was chopped into ~1 mm^3 pieces on ice and incubated shaking at 100 rpm at 37 °C with 5% CO_2 for 20 min. After passing through a 100 µm cell strainer (Spectrum) on ice, cells were collected at 400 x g for 10 min at 4°C. Leukocytes were separated by 40%/70% Percoll gradient, washed in PBS, resuspended in FACS buffer (PBS plus 1% BSA and 0.1% sodium azide), and stained with fluorophore-conjugated CD4 (1:100, clone GK 1.5, Biolegend), CD8 (1:100, clone 53-6.7, BD Pharmingen) and isotype controls. Cells were analyzed on Attune NxT Acoustic Focusing Cytometer (Life Technologies). Isotype and autofluorescence controls were examined for each assay. Acquired data were subsequently analyzed using FlowJo software (Treestar).

RNA isolation and qPCR

mRNA levels of cellular markers and cytokines in the spinal cord tissue during EAE progression were examined using qPCR as described earlier (Chechneva et al, 2011). Briefly, mice were anesthetized and perfused transcardially with ice cold PBS. Lumbar spinal cords were dissected and stored separately in liquid nitrogen. Total RNA was isolated from spinal cord tissue using Direct-zol RNA MiniPrep Kit (Zymo Research) following the standard protocol. RNA purity passed at the $OD_{260/280}$ ratio between 1.8 and 2.0. Total RNA (1 µg) was reverse-transcribed to cDNA using Multiscribe reverse transcriptase (Applied Biosystems). Subsequent qPCR reactions were performed in triplicates on a Roche LightCycler 480 using SYBR Green Master Mix (Roche Applied Science). Specific primers were designed using Primer3 Input software: *GAPDH*, forward: 5′-

GCCTTCCGTGTTCCTACC-3′, reverse: 5′-GCCTGCTTCACCACCTTC-3′; *CD45*, forward: 5′-GAAGATGTGGTTGATGTT-3′, reverse: 5′-GAACTGGTATTGCTCATAG-3′; *CD11b* (*Itgam* gene), forward: 5′-TCAGAAGATGAAGGAGTT-3′, reverse: 5′-CATTGAAGGTGAAGTGAA-3′. Product specificity for each primer set was validated by Tm melting curve analysis. TaqMan gene expression assays (Applied Biosystems) were used for *CD11c* (*Itgax* gene, Mm00498701_m1), *IL-6* (Mm00446190_m1), *CD4* (Mm00442754_m1), *CD8a* (Mm01182107_g1), *INF-γ* (Mm01168134_m1), *IL-17a* (Mm00439619_m1), *CD40* (Mm00441891_m1), *CD40LG* (Mm00441911_m1), *IL-12b* (Mm01288989_m1), *OPN* (*Spp1* gene, Mm00436767_m1), *CCR2* (Mm00438270_m1) and *CCL2* (Mm00441242_m1). All experimental samples were normalized to the expression level of *GAPDH* (4352339E Applied Biosystems). Relative quantification of fold-change was performed by applying the $2^{-\Delta\Delta}$Ct method and comparing Cp values of individual mice (Livak & Schmittgen, 2001).

Statistical analysis

Statistical analysis was performed using GraphPad Prism 5.0. EAE clinical scores were evaluated for statistical significance using Two-way ANOVA with Sidak's multiple comparisons test. One-way ANOVA with Tukey's post hoc test was used to analyze EAE values in Table 1. Two group differences were analyzed using Student's t-test. In all figures, data are represented as mean ± s.e.m. In all cases, probability values less than 0.05 were considered statistically significant. Images were assembled using Adobe Illustrator CC.

Author contributions

OVC designed and performed experiments, interpreted the data and wrote manuscript; FM performed experiments and wrote manuscript; ZD performed experiments; AZ performed experiments; DP edited manuscript; WD designed the study and edited manuscript.

Acknowledgments

We thank Dr. Peter Bannerman and Dr. Athena Soulika for comments and feedback on the project, Dr. Daniel Daugherty for help with EAE scoring. This work was in part supported by grants from National Institutes of Health (R01HD087566 and R01HD091325 to W.D.).

Conflict of interest

Authors declare no conflict of interest.

The paper explained

PROBLEM: MS is a chronic autoimmune demyelinating disease showing dynamic changes of clinical symptoms. While relapsing-remitting is the most common form of MS, progression of MS pathology and clinical symptoms occurs over time resulting in deterioration of neurologic function with no remission. MS is developing with higher prevalence in females than males, while in males disease progression is more rapid and severe. Approved immunosuppressive and immunomodulatory MS therapies reduce disease clinical symptoms and incidence of relapse but don't stop MS progression. To investigate molecular mechanism of MS progression and identify sex-specific therapeutic possibilities, an established animal model of MS, experimental autoimmune encephalomyelitis (EAE) is valuable.

RESULTS: In this study, we report that clinical progression of EAE in males is dependent on the activity of p38α MAPK signaling pathway in CD11c expressing cells. CD11c cell specific p38a deficiency blocked infiltration of peripheral immune cells into the spinal cord of male mice and thus, prevented EAE progression. Female mice with p38α deletion in CD11c+ cells were not protected from immune cell infiltration and progression of EAE clinical symptoms. Our data identified a sex-biased

mechanism in MS progression and provide useful information to advance effective strategies for MS treatment.

IMPACT: Our findings give explicit insight into cellular and molecular differences in MS pathology and progression between females and males. These data are meaningful and contribute to the development of new approaches for sex-specific MS therapies.

References

Ajami B, Bennett JL, Krieger C, McNagny KM, Rossi FM (2011) Infiltrating monocytes trigger EAE progression, but do not contribute to the resident microglia pool. Nat Neurosci 14**:** 1142-1149

Alliot F, Godin I, Pessac B (1999) Microglia derive from progenitors, originating from the yolk sac, and which proliferate in the brain. Brain Res Dev Brain Res 117**:** 145-152

Angele MK, Nitsch S, Knoferl MW, Ayala A, Angele P, Schildberg FW, Jauch KW, Chaudry IH (2003) Sex-specific p38 MAP kinase activation following trauma-hemorrhage: involvement of testosterone and estradiol. Am J Physiol Endocrinol Metab 285**:** E189-196

Babaloo Z, Aliparasti MR, Babaiea F, Almasi S, Baradaran B, Farhoudi M (2015) The role of Th17 cells in patients with relapsing-remitting multiple sclerosis: interleukin-17A and interleukin-17F serum levels. Immunol Lett 164**:** 76-80

Balashov KE, Smith DR, Khoury SJ, Hafler DA, Weiner HL (1997) Increased interleukin 12 production in progressive multiple sclerosis: induction by activated CD4+ T cells via CD40 ligand. Proceedings of the National Academy of Sciences of the United States of America 94**:** 599-603

Becher B, Durell BG, Miga AV, Hickey WF, Noelle RJ (2001) The clinical course of experimental autoimmune encephalomyelitis and inflammation is controlled by the expression of CD40 within the central nervous system. J Exp Med 193**:** 967-974

Bruemmer D, Collins AR, Noh G, Wang W, Territo M, Arias-Magallona S, Fishbein MC, Blaschke F, Kintscher U, Graf K et al (2003) Angiotensin II-accelerated atherosclerosis and aneurysm formation is attenuated in osteopontin-deficient mice. J Clin Invest 112**:** 1318-1331

Chastain EM, Duncan DS, Rodgers JM, Miller SD (2011) The role of antigen presenting cells in multiple sclerosis. Biochim Biophys Acta 1812**:** 265-274

Chechneva OV, Mayrhofer F, Daugherty DJ, Pleasure DE, Hong JS, Deng W (2011) Low dose dextromethorphan attenuates moderate experimental autoimmune encephalomyelitis by inhibiting NOX2 and reducing peripheral immune cells infiltration in the spinal cord. Neurobiol Dis 44**:** 63-72

Di Mitri D, Sambucci M, Loiarro M, De Bardi M, Volpe E, Cencioni MT, Gasperini C, Centonze D, Sette C, Akbar AN et al (2015) The p38 mitogen-activated protein kinase cascade modulates T helper type 17 differentiation and functionality in multiple sclerosis. Immunology 146**:** 251-263

Dogan RN, Elhofy A, Karpus WJ (2008) Production of CCL2 by central nervous system cells regulates development of murine experimental autoimmune encephalomyelitis through the recruitment of TNF- and iNOS-expressing macrophages and myeloid dendritic cells. J Immunol 180**:** 7376-7384

Fischer HG, Reichmann G (2001) Brain dendritic cells and macrophages/microglia in central nervous system inflammation. J Immunol 166**:** 2717-2726

Giachelli CM, Lombardi D, Johnson RJ, Murry CE, Almeida M (1998) Evidence for a role of osteopontin in macrophage infiltration in response to pathological stimuli in vivo. Am J Pathol 152**:** 353-358

Gold R, Linington C, Lassmann H (2006) Understanding pathogenesis and therapy of multiple sclerosis via animal models: 70 years of merits and culprits in experimental autoimmune encephalomyelitis research. Brain 129**:** 1953-1971

Gourraud PA, Harbo HF, Hauser SL, Baranzini SE (2012) The genetics of multiple sclerosis: an up-to-date review. Immunol Rev 248**:** 87-103

Greter M, Heppner FL, Lemos MP, Odermatt BM, Goebels N, Laufer T, Noelle RJ, Becher B (2005) Dendritic cells permit immune invasion of the CNS in an animal model of multiple sclerosis. Nat Med 11**:** 328-334

Haghikia A, Jorg S, Duscha A, Berg J, Manzel A, Waschbisch A, Hammer A, Lee DH, May C, Wilck N et al (2015) Dietary Fatty Acids Directly Impact Central Nervous System Autoimmunity via the Small Intestine. Immunity 43**:** 817-829

Heink S, Yogev N, Garbers C, Herwerth M, Aly L, Gasperi C, Husterer V, Croxford AL, Moller-Hackbarth K, Bartsch HS et al (2017) Trans-presentation of IL-6 by dendritic cells is required for the priming of pathogenic TH17 cells. Nat Immunol 18**:** 74-85

Herbert BA, Valerio MS, Gaestel M, Kirkwood KL (2015) Sexual Dimorphism in MAPK-Activated Protein Kinase-2 (MK2) Regulation of RANKL-Induced Osteoclastogenesis in Osteoclast Progenitor Subpopulations. PLoS One 10**:** e0125387

Herlaar E, Brown Z (1999) p38 MAPK signalling cascades in inflammatory disease. Mol Med Today 5**:** 439-447

Huang G, Wang Y, Vogel P, Kanneganti TD, Otsu K, Chi H (2012) Signaling via the kinase p38alpha programs dendritic cells to drive TH17 differentiation and autoimmune inflammation. Nat Immunol 13**:** 152-161

Huang Y, Xu Z, Xiong S, Sun F, Qin G, Hu G, Wang J, Zhao L, Liang YX, Wu T et al (2018) Repopulated microglia are solely derived from the proliferation of residual microglia after acute depletion. Nat Neurosci 21**:** 530-540

Hur EM, Youssef S, Haws ME, Zhang SY, Sobel RA, Steinman L (2007) Osteopontin-induced relapse and progression of autoimmune brain disease through enhanced survival of activated T cells. Nat Immunol 8**:** 74-83

Kaminska B, Mota M, Pizzi M (2016) Signal transduction and epigenetic mechanisms in the control of microglia activation during neuroinflammation. Biochim Biophys Acta 1862**:** 339-351

Kim C, Sano Y, Todorova K, Carlson BA, Arpa L, Celada A, Lawrence T, Otsu K, Brissette JL, Arthur JS et al (2008) The kinase p38 alpha serves cell type-specific inflammatory functions in skin injury and coordinates pro- and anti-inflammatory gene expression. Nat Immunol 9**:** 1019-1027

Kim RY, Hoffman AS, Itoh N, Ao Y, Spence R, Sofroniew MV, Voskuhl RR (2014) Astrocyte CCL2 sustains immune cell infiltration in chronic experimental autoimmune encephalomyelitis. J Neuroimmunol 274**:** 53-61

Krementsov DN, Noubade R, Dragon JA, Otsu K, Rincon M, Teuscher C (2014) Sex-specific control of central nervous system autoimmunity by p38 mitogen-activated protein kinase signaling in myeloid cells. Ann Neurol 75**:** 50-66

Krementsov DN, Thornton TM, Teuscher C, Rincon M (2013) The emerging role of p38 mitogen-activated protein kinase in multiple sclerosis and its models. Mol Cell Biol 33**:** 3728-3734

Larochelle C, Alvarez JI, Prat A (2011) How do immune cells overcome the blood-brain barrier in multiple sclerosis? FEBS Lett 585**:** 3770-3780

Li R, Sun X, Shu Y, Mao Z, Xiao L, Qiu W, Lu Z, Hu X (2017) Sex differences in outcomes of disease-modifying treatments for multiple sclerosis: A systematic review. Mult Scler Relat Disord 12**:** 23-28

Livak KJ, Schmittgen TD (2001) Analysis of relative gene expression data using real-time quantitative PCR and the 2(-Delta Delta C(T)) Method. Methods 25**:** 402-408

Lo U, Selvaraj V, Plane JM, Chechneva OV, Otsu K, Deng W (2014) p38alpha (MAPK14) critically regulates the immunological response and the production of specific cytokines and chemokines in astrocytes. Sci Rep 4**:** 7405

Merad M, Sathe P, Helft J, Miller J, Mortha A (2013) The dendritic cell lineage: ontogeny and function of dendritic cells and their subsets in the steady state and the inflamed setting. Annu Rev Immunol 31**:** 563-604

Molnarfi N, Schulze-Topphoff U, Weber MS, Patarroyo JC, Prod'homme T, Varrin-Doyer M, Shetty A, Linington C, Slavin AJ, Hidalgo J et al (2013) MHC class II-dependent B cell APC function is required for induction of CNS autoimmunity independent of myelin-specific antibodies. J Exp Med 210**:** 2921-2937

Moreno M, Bannerman P, Ma J, Guo F, Miers L, Soulika AM, Pleasure D (2014) Conditional ablation of astroglial CCL2 suppresses CNS accumulation of M1 macrophages and preserves axons in mice with MOG peptide EAE. J Neurosci 34**:** 8175-8185

Moreno MA, Burns T, Yao P, Miers L, Pleasure D, Soulika AM (2016) Therapeutic depletion of monocyte-derived cells protects from long-term axonal loss in experimental autoimmune encephalomyelitis. J Neuroimmunol 290**:** 36-46

Orthgiess J, Gericke M, Immig K, Schulz A, Hirrlinger J, Bechmann I, Eilers J (2016) Neurons exhibit Lyz2 promoter activity in vivo: Implications for using LysM-Cre mice in myeloid cell research. Eur J Immunol 46**:** 1529-1532

Owens T, Bechmann I, Engelhardt B (2008) Perivascular spaces and the two steps to neuroinflammation. J Neuropathol Exp Neurol 67**:** 1113-1121

Pashenkov M, Efendic S, Zhu J, Zou LP, Ostenson CG, Mustafa M (2000) Augmented expression of daintain/allograft inflammatory factor-1 is associated with clinical disease: dynamics of daintain/allograft inflammatory factor-1 expression in spleen, peripheral nerves and sera during experimental autoimmune neuritis. Scand J Immunol 52**:** 117-122

Prodinger C, Bunse J, Kruger M, Schiefenhovel F, Brandt C, Laman JD, Greter M, Immig K, Heppner F, Becher B et al (2011) CD11c-expressing cells reside in the juxtavascular parenchyma and extend processes into the glia limitans of the mouse nervous system. Acta Neuropathol 121**:** 445-458

Rahn EJ, Iannitti T, Donahue RR, Taylor BK (2014) Sex differences in a mouse model of multiple sclerosis: neuropathic pain behavior in females but not males and protection from neurological deficits during proestrus. Biol Sex Differ 5**:** 4

Romme Christensen J, Bornsen L, Ratzer R, Piehl F, Khademi M, Olsson T, Sorensen PS, Sellebjerg F (2013) Systemic inflammation in progressive multiple sclerosis involves follicular T-helper, Th17- and activated B-cells and correlates with progression. PLoS One 8**:** e57820

Serafini B, Columba-Cabezas S, Di Rosa F, Aloisi F (2000) Intracerebral recruitment and maturation of dendritic cells in the onset and progression of experimental autoimmune encephalomyelitis. Am J Pathol 157**:** 1991-2002

Shi LZ, Wang R, Huang G, Vogel P, Neale G, Green DR, Chi H (2011) HIF1alpha-dependent glycolytic pathway orchestrates a metabolic checkpoint for the differentiation of TH17 and Treg cells. J Exp Med 208**:** 1367-1376

Taves S, Berta T, Liu DL, Gan S, Chen G, Kim YH, Van de Ven T, Laufer S, Ji RR (2016) Spinal inhibition of p38 MAP kinase reduces inflammatory and neuropathic pain in male but not female mice: Sex-dependent microglial signaling in the spinal cord. Brain, behavior, and immunity 55**:** 70-81

Tran EH, Hoekstra K, van Rooijen N, Dijkstra CD, Owens T (1998) Immune invasion of the central nervous system parenchyma and experimental allergic encephalomyelitis, but not leukocyte extravasation from blood, are prevented in macrophage-depleted mice. J Immunol 161**:** 3767-3775

Vogt MH, Floris S, Killestein J, Knol DL, Smits M, Barkhof F, Polman CH, Nagelkerken L (2004) Osteopontin levels and increased disease activity in relapsing-remitting multiple sclerosis patients. J Neuroimmunol 155**:** 155-160

Voskuhl RR, Gold SM (2012) Sex-related factors in multiple sclerosis susceptibility and progression. Nat Rev Neurol 8**:** 255-263

Wang J, Syrett CM, Kramer MC, Basu A, Atchison ML, Anguera MC (2016) Unusual maintenance of X chromosome inactivation predisposes female lymphocytes for increased expression from the inactive X. Proceedings of the National Academy of Sciences of the United States of America 113**:** E2029-2038

Wentworth JM, Naselli G, Brown WA, Doyle L, Phipson B, Smyth GK, Wabitsch M, O'Brien PE, Harrison LC (2010) Pro-inflammatory CD11c+CD206+ adipose tissue macrophages are associated with insulin resistance in human obesity. Diabetes 59**:** 1648-1656

Yanagawa Y, Onoe K (2006) Distinct regulation of CD40-mediated interleukin-6 and interleukin-12 productions via mitogen-activated protein kinase and nuclear factor kappaB-inducing kinase in mature dendritic cells. Immunology 117**:** 526-535

Zarubin T, Han J (2005) Activation and signaling of the p38 MAP kinase pathway. Cell Res 15**:** 11-18

Figure legends

Fig. 1. Knockout of *p38α* in CD11c^{+} cells prevents EAE progression in male mice. *p38α*$^{fl/fl}$ and p38αΔCD11c female and male mice were immunized with MOG-PTX to induce EAE. EAE clinical scores were monitored daily through day 60 post immunization (A). Data are representative of four independent experiments with n = 47 for p38α$^{\Delta CD11c}$ males, n = 39 for p38α$^{\Delta CD11c}$ females, n = 41 for p38α$^{fl/fl}$ males and n = 32 for p38α$^{fl/fl}$ females. *P* values were determined by two-way ANOVA with Sidak's multiple comparisons test; *, $P < 0.05$. H&E (B) and LFB (C) staining of the lumbar spinal cord of *p38α*$^{\Delta CD11c}$ male and female mice at EAE progression in females (day 32 post immunization). Immunostaining for MBP co-stained with DAPI (D). Scale bar 100 µm for B-C, 50 µm for D. EAE pathological score based on the degree of infiltration and demyelination (E). Data are representative of two independent experiments. *P* value was determined by Student's t-test.

Fig. 2. Knockout of *p38α* in CD11c^{+} cells in males prevents T cell infiltration. CD4^{+} T cells in the lumbar spinal cord of *p38α*$^{\Delta CD11c}$ male (A) and female (B) mice at EAE progression in females (day 32 post immunization). Pattern of CD4^{+} cell distribution in the dorsal spinal cord (A-B, enlargements). Scale bars 200 µm for A-B, 20 µm for enlargements. Number of CD4^{+} cells in the spinal cord white matter (C). Flow cytometry analysis of CD4^{+} and CD8^{+} cells in the CNS of *p38α*$^{\Delta CD11c}$ male and female mice at EAE progression in females (D). Percentage of CD4^{+} and CD8^{+} cells analyzed by FACS (E). mRNA transcription level of *CD4* and *CD8a* in the lumbar spinal cord (F). mRNA transcription level of *INF-γ* and *IL-17a* in the lumbar spinal cord (G). mRNA transcription level of *IL-12b* (H) and *IL-6* (I) in the lumbar spinal cord at EAE progression in females. Data are representative of two independent experiments. *P* value was determined by Student's t-test. Each circle represents an individual mouse and small horizontal line indicates the mean. NS, not significant.

Fig. 3. Knockout of *p38α* in CD11c$^+$ cells in males prevents invasion of macrophages. Iba1$^+$ cells in the lumbar spinal cord of *p38α*$^{\Delta CD11c}$ male (A) and female (B) mice at EAE progression in females (day 32 post immunization). Iba1$^+$ cells in the lateral and ventral spinal cord (A-B, enlargements). Infiltrating lectin$^+$ macrophages and CD4$^+$ T cells in the ventral lumbar spinal cord of *p38α*$^{\Delta CD11c}$ male (C) and female (D) mice at EAE progression. Pattern of CD45$^+$ cell infiltration in male (E) and female (F) mice at EAE progression. Scale bars 200 µm for A-B, 20 µm for enlargements in A-B; 50 µm for C-F. mRNA transcription level of *CD45* (G) and *CD11b* (encoded by *Itgam* gene) (H) in the lumbar spinal cord. Data are representative of two independent experiments. *P* value was determined by Student's t-test.

Fig. 4. CD11c$^+$CD11b$^+$Iba1$^+$ cells are involved in EAE progression in *p38α*$^{\Delta CD11c}$ females. CD11c$^+$ cells were detected using *CD11c*-promoter driven expression of eGFP. In males, eGFP$^+$ cells co-expressing CD11b clustered at the meninges (A). eGFP$^+$ microglia (arrows) and microglia with dendritic cell morphology (A, arrow head and enlargement) in ventral white matter of *p38α*$^{\Delta CD11c}$ males. eGFP$^+$CD11b$^+$ and CD11b$^+$ cells with macrophage/reactive microglia morphology in the spinal cord parenchyma of *p38α*$^{\Delta CD11c}$ females (B). eGFP$^+$ cells co-expressed macrophage/microglia marker Iba1 (C, D). Scale bars 20 µm for A, B; 10 µm for A, C enlargement; 50 µm for C, D; 25 µm for B, D enlargements. mRNA transcription level of *CD11c* (encoded by *Itgax* gene) in the lumbar spinal cord at EAE progression in females (E). Data are representative of two independent experiments. *P* value was determined by Student's t-test.

Fig. 5. Macrophages/reactive microglia upregulate CD40 and MHC-II in *p38α*$^{\Delta CD11c}$ female mice. Transcription level of *CD40LG* (A) and *CD40* (B) in the lumbar spinal cord of *p38α*$^{\Delta CD11c}$ males and

females at EAE progression. Data are representative of two independent experiments. *P* value was determined by Student's t-test. Expression of CD40 in ventral (C, E) and dorsal (D, F) lumbar spinal cord of male and female *p38α*$^{\Delta CD11c}$ mice at EAE progression in females. In males, MHC-II^{+} cells accumulated at the meninges (G). eGFP^{+}MHC-II^{+}Iba1^{-} DC in the perivascular space (G, arrow). eGFP^{+}Iba1^{+} DC-like microglia show low MHC-II expression (G, star). Some eGFP^{+}Iba1^{+}MHC-II^{-} (G, pound) and eGFP^{+}MHC-II^{-}Iba1^{-} cells are found in the parenchyma in males (G, arrowhead). In females, eGFP^{+} cells co-expressing MHC-II and Iba1 found in the perivascular space and spinal cord parenchyma (H). Scale bars 100 µm for C, E; 10 µm for D-H.

Fig. 6. Astrocyte-derived OPN and CCL2 mediate EAE progression in *p38α*$^{\Delta CD11c}$ females. Expression of OPN in *p38α*$^{\Delta CD11c}$ male and female lumbar spinal cord at EAE progression in females (A, B). mRNA transcription level of *OPN* (encoded by *Spp1* gene) in the lumbar spinal cords at EAE progression (C). OPN expression localized to GFAP^{+} astrocytes in the spinal cords of *p38α*$^{\Delta CD11c}$ males (D) and females (E). OPN^{+} cells with OPC morphology found in the spinal cords of male mice (D, arrow). Note reactive phenotype of GFAP^{+} astrocytes in female spinal cord at EAE progression. In males, CCL2^{+} astrocytes found in spinal cord parenchyma (F). CCL2 expression is upregulated in reactive astrocytes in females (G). Scale bars 20 µm for A-B; 10 µm for D-E, F-G. mRNA transcription level of *CCL2* (H) and *CCR2* (I) in the lumbar spinal cords at EAE progression. Data are representative of two independent experiments. *P* value was determined by Student's t-test.

Table 1. EAE clinical characteristics in *p38α*$^{fl/fl}$ and *p38α*$^{\Delta CD11c}$ female and male mice

Group	n	Onset	Mean score 1st peak	Mean score d26	Mean score d32	Max severity from d29	Duration of paralysis d29 – d60	Score at d60	Survival
p38α$^{\Delta CD11c}$ females	39	14.1 ± 0.5$^{\#\#}$	3.2 ± 0.2	2.4 ± 0.2	2.9 ± 0.2$^{\#}$	3.3 ± 0.2$^{\#}$	17.2 ± 2.3	2.9 ± 0.2$^{\#}$	94.9%
p38α$^{\Delta CD11c}$ males	47	12.2 ± 0.3	3.3 ± 0.1	2.2 ± 0.2	2.1 ± 0.2	2.7 ± 0.2	10.0 ± 2.1	2.1 ± 0.2	95.7%
p38α$^{fl/fl}$ females	32	12.4 ± 0.4*	4.0 ± 0.1***	3.2 ± 0.2**	3.3 ± 0.2	3.7 ± 0.2	23.9 ± 2.3*	3.4 ± 0.2	90.6%
p38α$^{fl/fl}$ males	41	11.2 ± 0.2	4.2 ± 0.1***	3.2 ± 0.2***	3.4 ± 0.2***	3.9 ±0.1***	25.9 ± 1.8***	3.7 ± 0.2***	90.2%

Data represent the mean ± s.e.m. **P*<0.05, ***P*<0.01, ****P*<0.001, comparing between same sex p38α$^{fl/fl}$ and p38α$^{\Delta CD11c}$ mice. $^{\#\#}$*P*<0.01, comparing between females and males of same genotype (One-way ANOVA with Tukey's post hoc).

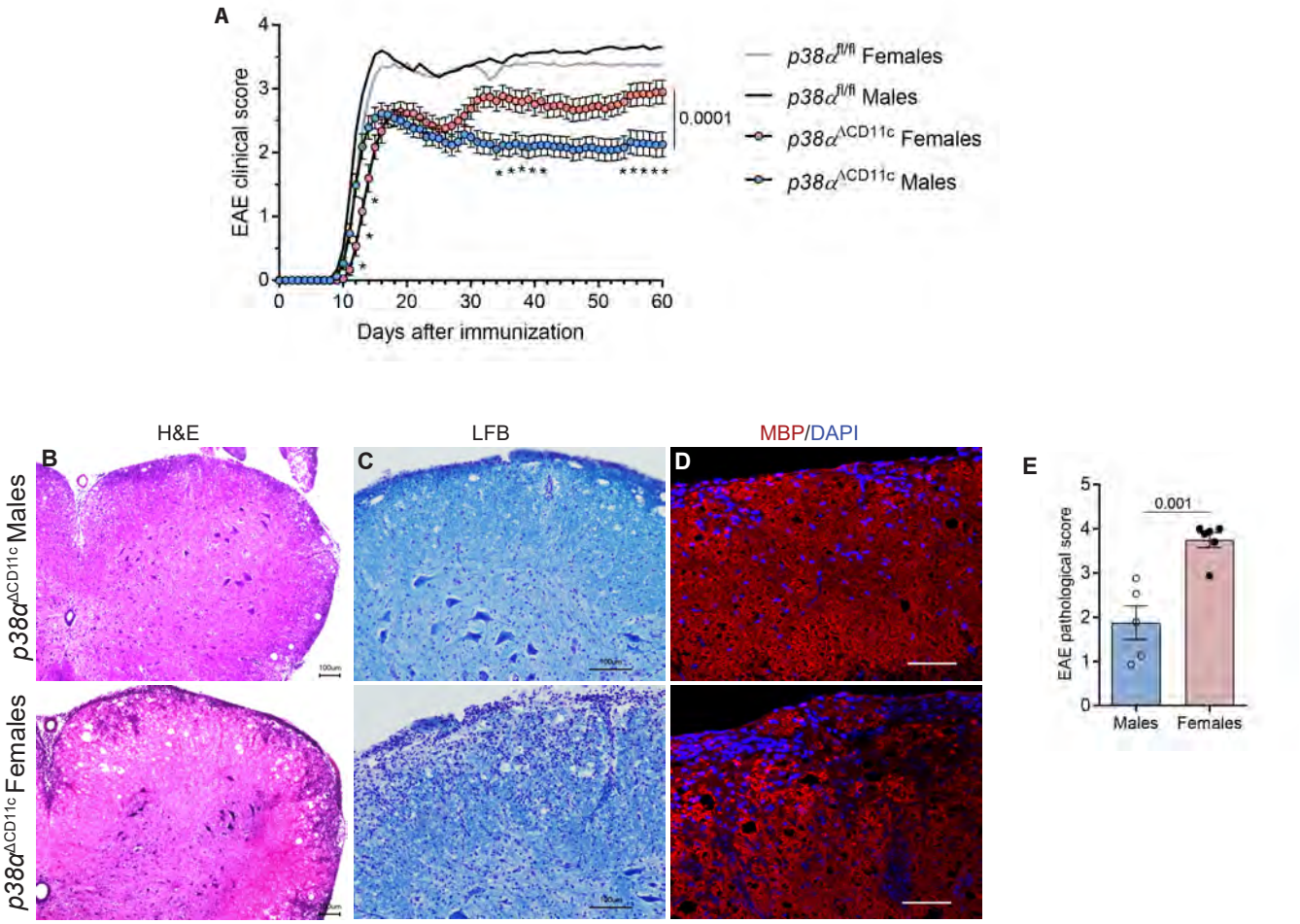
A
EAE clinical score
Days after immunization
0.0001
p38α fl/fl Females
p38α fl/fl Males
p38α ΔCD11c Females
p38α ΔCD11c Males
H&E
LFB
MBP/DAPI
B
C
D
E
p38α ΔCD11c Males
p38α ΔCD11c Females
EAE pathological score
0.001
Males
Females

Fig 1

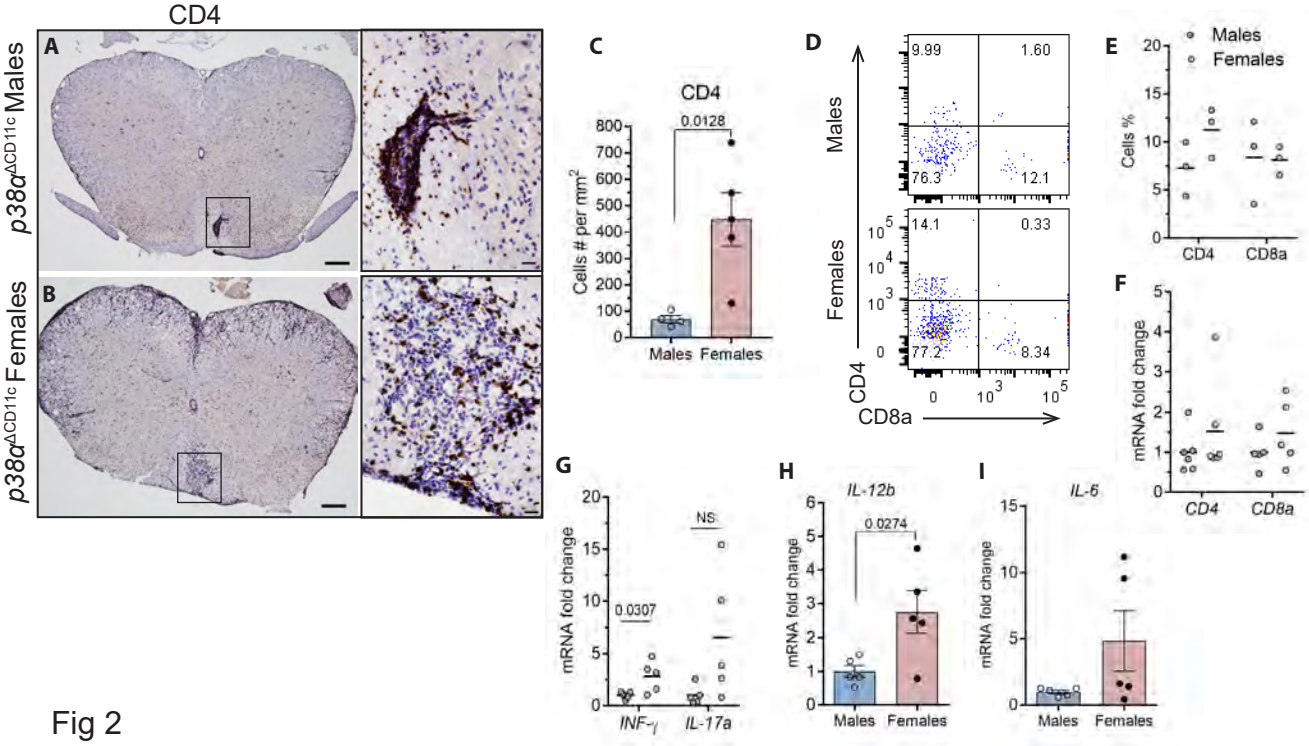
CD4
A
B
p38α^ΔCD11c Males
p38α^ΔCD11c Females
C
CD4
0.0128
Cells # per mm²
Males
Females
D
Males
Females
9.99
1.60
76.3
12.1
14.1
0.33
77.2
8.34
CD4
CD8a
E
Males
Females
Cells %
CD4
CD8a
F
mRNA fold change
CD4
CD8a
G
mRNA fold change
0.0307
NS
INF-γ
IL-17a
H
IL-12b
0.0274
mRNA fold change
Males
Females
I
IL-6
mRNA fold change
Males
Females

Fig 2

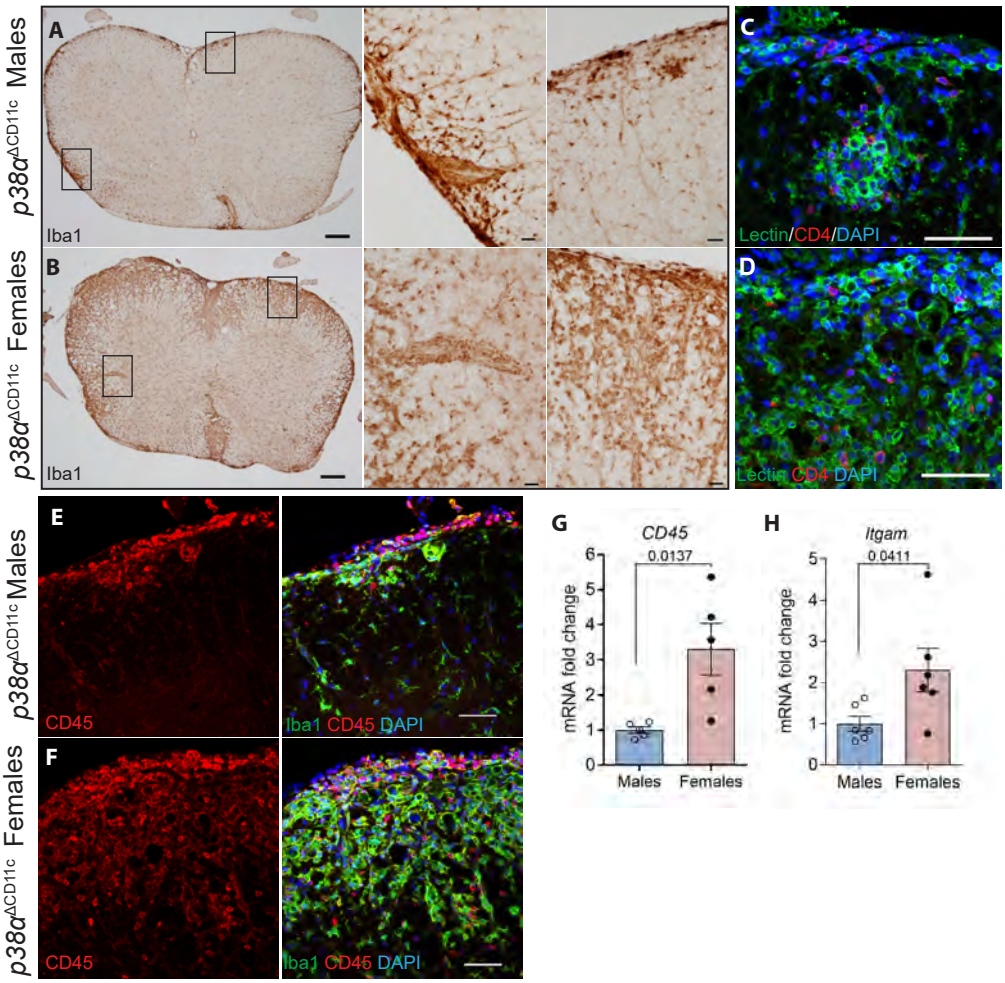
p38α ΔCD11c Males
p38α ΔCD11c Females
A
B
C
D
E
F
G
H
Iba1
Lectin/CD4/DAPI
CD45
Iba1 CD45 DAPI
CD45
0.0137
mRNA fold change
Males
Females
Itgam
0.0411
mRNA fold change
Males
Females

Fig 3

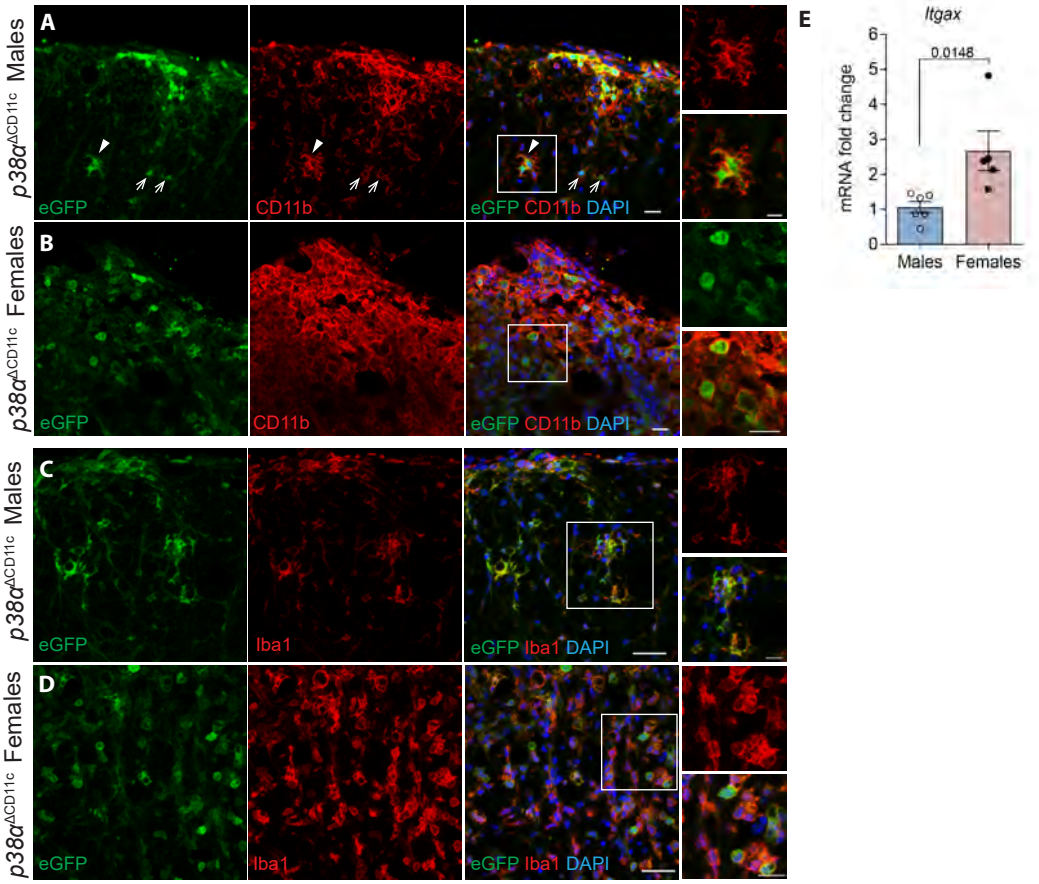
A
Males
p38α ΔCD11c
eGFP
CD11b
eGFP CD11b DAPI
B
Females
p38α ΔCD11c
eGFP
CD11b
eGFP CD11b DAPI
C
Males
p38α ΔCD11c
eGFP
Iba1
eGFP Iba1 DAPI
D
Females
p38α ΔCD11c
eGFP
Iba1
eGFP Iba1 DAPI
E
Itgax
mRNA fold change
0.0148
0
1
2
3
4
5
6
Males
Females

Fig 4

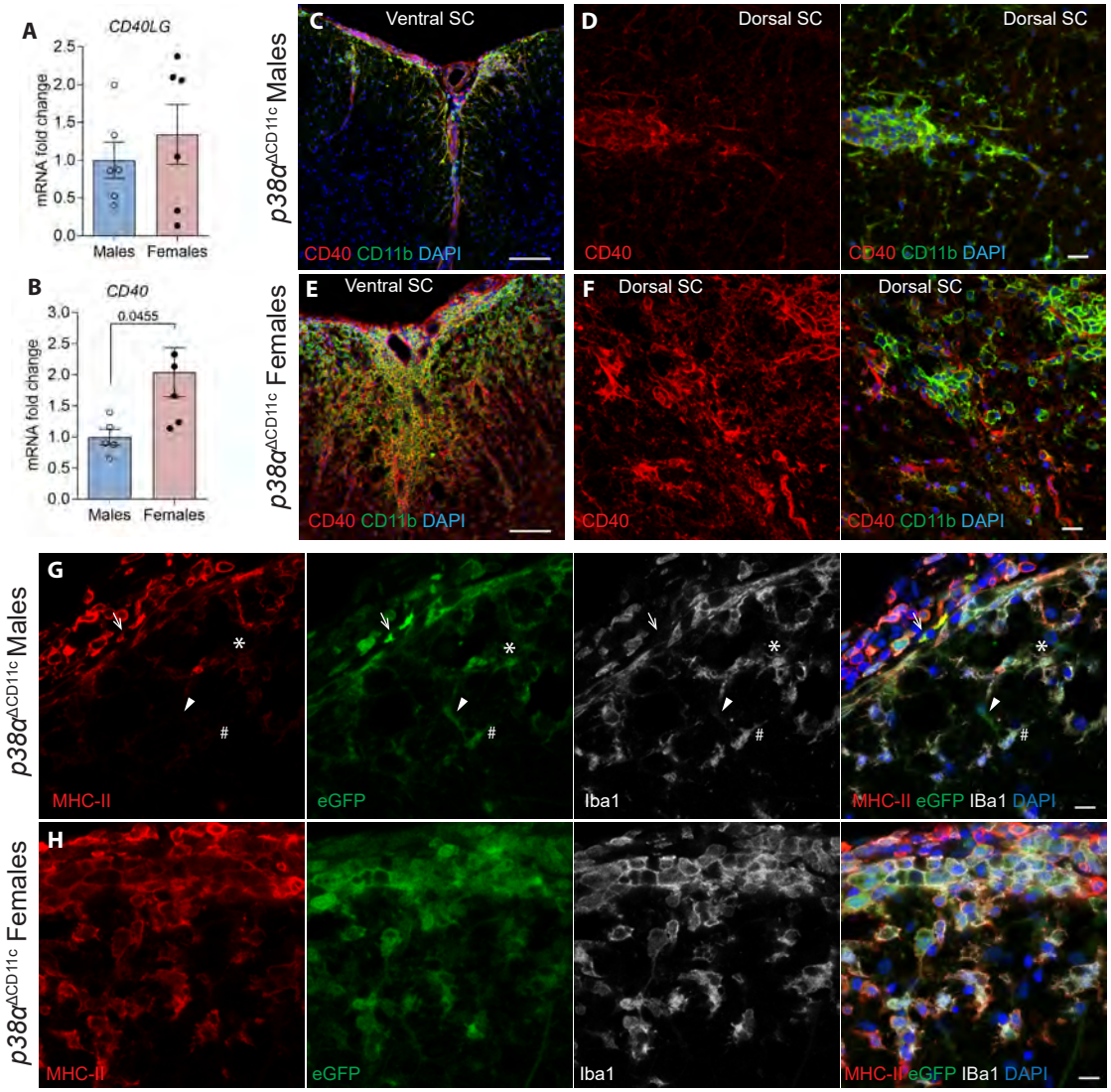
A
CD40LG
mRNA fold change
2.5
2.0
1.5
1.0
0.5
0.0
Males
Females
B
CD40
0.0455
mRNA fold change
3.0
2.5
2.0
1.5
1.0
0.5
0.0
Males
Females
p38α^ΔCD11c Males
p38α^ΔCD11c Females
C
Ventral SC
CD40 CD11b DAPI
D
Dorsal SC
CD40
Dorsal SC
CD40 CD11b DAPI
E
Ventral SC
CD40 CD11b DAPI
F
Dorsal SC
CD40
Dorsal SC
CD40 CD11b DAPI
G
MHC-II
eGFP
Iba1
MHC-II eGFP IBa1 DAPI
H
MHC-II
eGFP
Iba1
MHC-II eGFP IBa1 DAPI

Fig 5

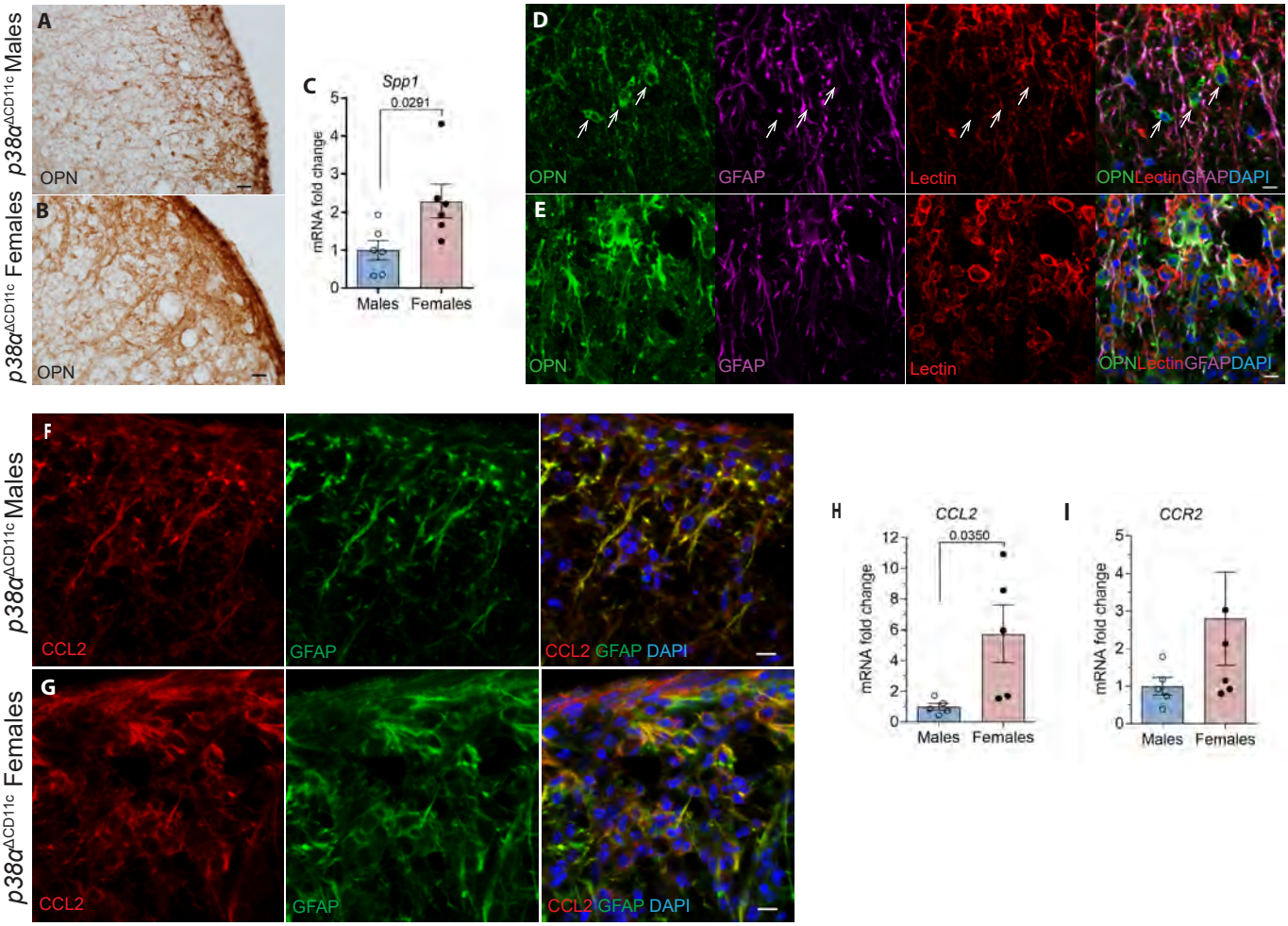
p38α^ΔCD11c Males
p38α^ΔCD11c Females
A
OPN
B
OPN
C
Spp1
0.0291
mRNA fold change
Males
Females
D
OPN
GFAP
Lectin
OPNLectinGFAPDAPI
E
OPN
GFAP
Lectin
OPNLectinGFAPDAPI
F
CCL2
GFAP
CCL2 GFAP DAPI
G
CCL2
GFAP
CCL2 GFAP DAPI
H
CCL2
0.0350
mRNA fold change
Males
Females
I
CCR2
mRNA fold change
Males
Females

Fig 6